Int. J. Therm. Sci. (2001) 40, 899–910

S1290-0729(01)01276-5/FLA

Transient natural convection in an enclosure with horizontal temperature and vertical solutal gradients

Rachid Bennacer [a], Abdulmajeed A. Mohamad [b,*], Dalila Akrour [c]

[a] *Laboratoire Matériaux et Sciences des Constructions, Rue d'Eragny, 95031 Neuville sur Oise, France*

[b] *Department of Mechanical Engineering, 2500 University Drive, Calgary, AB, Canada T2N 1N4*

[c] *Laboratoire de Mécanique des Fluides, Institut de physique, U.S.T.H.B., B.P. 32 El-Alia, Bab-Ezzouar 16111, Algeria*

(Received 12 June 2000, accepted 8 December 2000)

Abstract — Transient, double diffusive natural convection in a horizontal enclosure is investigated numerically and analytically. The enclosure is heated and cooled along the vertical walls and solutal gradient is imposed vertically. The objective of the work is to identify the flow regime for thermal and solutal dominated flows. It is found that the flow becomes unstable (oscillatory) for finite range of solutal to thermal buoyancy ratios. It is possible to obtain different solutions on this region depending on the initial conditions. Also, the results reveal that the thermal convection may be suppressed for strongly stratified fluid. Owing to the large number of parameters, the results are reported for aspect ratio of two, Prandtl number of 7.0 (water) and Lewis number of 100 (aqueous solution). Rayleigh number is varied between 7×10^3 and 7×10^5. © 2001 Éditions scientifiques et médicales Elsevier SAS

double diffusive convection / horizontal en closure / unstable flow / numerical / analytical

Nomenclature

A	aspect ratio $= L/H$	
C	dimensional solute concentration . . .	$\mathrm{kg{\cdot}kg^{-1}}$ or wt%
D	mass diffusivity	$\mathrm{m^2{\cdot}s^{-1}}$
F_S	solutal buoyancy force	N
F_T	thermal buoyancy force	N
g	gravitational acceleration	$\mathrm{m{\cdot}s^{-2}}$
Gr_S	solutal Grashof number $= g\beta_S \Delta C H^3/\nu^2$	
Gr_T	thermal Grashof number $= g\beta_T \Delta T H^3/\nu^2$	
H, L	height and length of the enclosure	
Le	Lewis number $= \alpha/D$	
N	buoyancy ratio $= \beta_S \Delta C/\beta_T \Delta T$	
Nu	average Nusselt number $= \int_0^1 (\partial\theta/\partial\xi)_{\xi=0}\,\mathrm{d}\eta$	
P	dimensionless pressure	
Pr	Prandtl number $= \nu/\alpha$	
Ra_T	thermal Rayleigh number $= Gr_T Pr$	
Sc	Schmidt number $= \nu/D$	
Sh	Average Sherwood number $= (1/A)\int_0^1 (\partial\phi/\partial X)_{X=0}\,\mathrm{d}Z$	
T	dimensional temperature	K
$u(v)$	horizontal (vertical) components of the velocity	$\mathrm{m{\cdot}s^{-1}}$
$U(V)$	horizontal (vertical) dimensionless components of velocity $= uH/\nu$ $(= vH/\nu)$	
x, y	coordinate system	m

Greek symbols

α	thermal diffusivity	$\mathrm{m^2{\cdot}s^{-1}}$
β_S	coefficient of density change due to concentration	$\%\mathrm{wt}^{-1}$
β_T	coefficient of volumetric thermal expansion	K^{-1}
$\eta(\xi)$	dimensionless coordinate system $= y/H$ $(= x/H)$	
ϕ	dimensionless concentration $= (C - C_o)/\Delta C$	
θ	dimensionless temperature $= (T - T_o)/\Delta T$	
ΔC	concentration difference between horizontal boundaries $= C_h - C_l$	$\mathrm{kg{\cdot}kg^{-1}}$
ΔT	temperature difference between vertical boundaries $= T_h - T_c$	K

* Correspondence and reprints.
E-mail address: amohamad@enme.ucalgary.ca (A.A. Mohamad).

μ	dynamic viscosity of the fluid	$kg{\cdot}m^{-1}{\cdot}s^{-1}$
ν	kinematics viscosity	$m^2{\cdot}s^{-1}$
ρ	fluid density	$kg{\cdot}m^{-3}$

Subscript

c	cold
h	hot or high
l	low
o	reference state
S	solutal
T	thermal

1. INTRODUCTION

Double diffusive natural convection is well reviewed by Bejan [1]. Most of the work done on the double diffusive natural convection is focused on differentially heated (horizontal gradients) enclosures with aiding or opposing solutal gradient. Recently, there has been a focus on transient regime (Krishnan [2], Zhou and Zebib [3], Gobin and Bennacer [4], Kamakura and Ozoe [5] and Nishimura, Imoto et al. [6]) in order to understand the oscillatory regime which occurs for a certain range of buoyancy ratio (transitional flow from cooperating to opposing).

As far as authors knowledge is concerned, no work is cited on imposed cross relation between temperature and concentration gradient (temperature–concentration gradient is imposed vertically and concentration–temperature gradient is imposed horizontally), which is the subject of this work. It should mention that Mohamad and Bennacer [7] reported cross relation between temperature and solutal gradient in an enclosure filled with saturated porous media. Stable or unstable stratification takes place in an enclosure subjected to positive or negative solutal gradients, respectively. Stable stratification produces a linear diffusive gradient in the vertical direction and any perturbation in the initial or boundary conditions may be suppressed due to stratification. But, for unstable stratification (high solutal concentration on the top of low concentration), perturbation in the initial or boundary conditions may amplify and flow initiates in the cavity. Rolls or plums form above a threshold solutal Rayleigh number (solutal Rayleigh–Bénard problem), i.e., the flow structure depends on the solutal Rayleigh number, geometry of the container and fluid properties. The flow structure becomes quite complex and a two-dimensional solution is difficult to justify. On the other hand, if a temperature gradient is imposed horizontally (differential heating), it may rearrange the structure of the flow, which depends on the thermal Rayleigh number and two dimensional solution may be justified. It is worth mentioning that imposing horizontal temperature gradient may have similar effect of tilting the enclosure or shearing the lid of the cavity. Based on the above argument, two-dimensional solution can be justified for cross gradient status. However, two-dimensional flow may be not suitable approximation for unsteady and high Grashof number, this issue is under investigation. This problem has fundamental importance as well as application in oceanography and chemical deposition. For instance, in renewable energy storage in stabily stratified (salt solution) pool subjected to solar heating is efficient if the convection is prevented. Understanding the criteria for the onset of convection is very important in such a problem in order to improve thermal energy storage systems.

Another problem seems to be equivalent which concerns the lateral heating of stabily stratified salt solution. In these kinds of problems the criteria of the onset of layered convection and size of cells was the main objective of the following authors (Thorpe et al. [8], Wirtz and Reddy [9], Bénard et al. [10], Chen and Liu [11] and Dijkstra and Kranenborg [12]). The problem under consideration is different from the previously investigated problems because the solutal boundary is imposed and steady state solution presented.

The paper focuses on the analysis of the flow, heat and mass transfer in a horizontal cavity of aspect ratio of two and for a range of Rayleigh number. Prandtl number is fixed to 7.0 and *Le* to 100 (aqueous solution). The work is concentrated on stable stratified flow. Interesting results are obtained for a wide range of solutal to thermal buoyancy ratios.

2. MATHEMATICAL AND NUMERICAL FORMULATION

2.1. Mathematical model

The physical model and coordinate system are shown in *figure 1*. The geometry under consideration is a two-dimensional horizontal enclosure of height H and width L. The vertical walls of the enclosure are subjected to temperature T_h and T_c at the vertical left and the right walls, respectively. The horizontal surfaces are subjected to a fixed concentration, high concentration at the bottom (C_h) and low concentration (C_l) at the top boundaries. It is assumed that the flow is incompressible, laminar and binary fluid is Newtonian. The thermophysical propri-

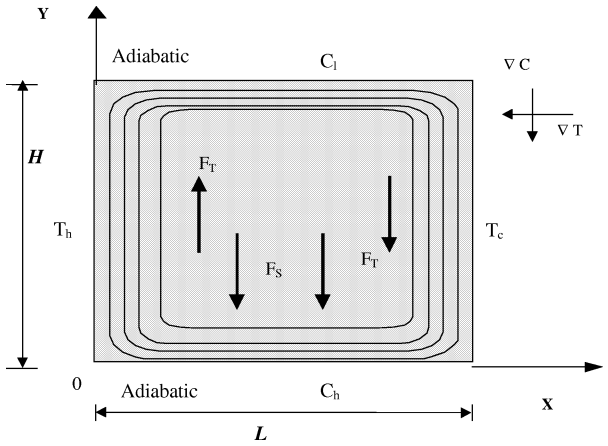

Figure 1. Schematic diagram and the coordinate system for convection with horizontal temperature and vertical solutal gradient.

eties of the fluid are assumed to be constants, except density in the buoyancy term, which depends linearly on both the local temperature and concentration, i.e., Boussinesq approximation is assumed to be valid,

$$\rho(T,C) = \rho_o\left[1 - \beta_T(T - T_o) - \beta_S(C - C_o)\right] \quad (1)$$

where, $\beta_T = -1/\rho_o[\partial\rho/\partial T]_C$ and $\beta_S = -1/\rho_o[\partial\rho/\partial C]_T$.

Soret and Dufour effects on heat and mass diffusion are neglected, nevertheless the Soret effect can modify the buoyancy value for which the instabilities are observed. Holinger and Lücke [13] found that Soret effect has an influence on the onset of double diffusive convection in a cavity subjected to horizontal temperature and concentration gradients.

The height of the cavity (H) is taken as a reference length for the spatial coordinates ($\xi = x/H$ and $\eta = y/H$). The references for time, velocity, pressure, temperature and species concentration are defined as H^2/ν, ν/H, $\rho\nu^2/H^2$, ΔT and ΔC, respectively.

The dimensionless macroscopic conservation equations of mass, momentum, energy and species can be written as follow:

Continuity

$$\frac{\partial U}{\partial \xi} + \frac{\partial V}{\partial \eta} = 0 \quad (2)$$

Momentum

$$\frac{\partial U}{\partial \tau} + U\frac{\partial U}{\partial \xi} + V\frac{\partial U}{\partial \eta} = \frac{\partial P}{\partial \xi} + \nabla^2 U \quad (3a)$$

$$\frac{\partial V}{\partial \tau} + U\frac{\partial V}{\partial \xi} + V\frac{\partial V}{\partial \eta} = \frac{\partial P}{\partial \xi} + \nabla^2 V + Gr_T(\theta + N\phi) \quad (3b)$$

Energy

$$\frac{\partial \theta}{\partial \tau} + U\frac{\partial \theta}{\partial \xi} + V\frac{\partial \theta}{\partial \eta} = \frac{1}{Pr}\nabla^2\theta \quad (4)$$

Species transport equation

$$\frac{\partial \phi}{\partial \tau} + U\frac{\partial \phi}{\partial \xi} + V\frac{\partial \phi}{\partial \eta} = \frac{1}{Pr\,Le}\nabla^2\phi \quad (5)$$

The dimensionless parameters that characterize the physics of the problem are the aspect ratio of the cavity $A = L/H$, the Prandtl number $Pr = \nu/\alpha$, the Schmidt number $Sc = \nu/D$, the thermal Grashof number $Gr_T = (\beta_T g \Delta T H^3)/\nu^2$ and the solutal to thermal buoyancy ratio N.

The boundary conditions for the governing equations are the non-slip condition at the impermeable walls. The constant temperatures are adopted along the vertical walls and adiabatic condition on the horizontal walls. The constant species concentrations are adopted along the horizontal walls and zero mass fluxes at the vertical walls of the enclosure. Hence,

$$U = V = 0, \quad \theta = 0.5, \quad \frac{\partial \phi}{\partial \xi} = 0 \quad \text{at } \xi = 0 \quad (6a)$$

$$U = V = 0, \quad \theta = -0.5, \quad \frac{\partial \phi}{\partial \xi} = 0 \quad \text{at } \xi = A \quad (6b)$$

$$U = V = 0, \quad \frac{\partial \theta}{\partial \eta} = 0, \quad \phi = 0.5 \quad \text{at } \eta = 0 \quad (6c)$$

$$U = V = 0, \quad \frac{\partial \theta}{\partial \eta}, \quad \phi = -0.5 \quad \text{at } \eta = 1 \quad (6d)$$

The average rate of heat and mass transfer across the vertical and horizontal walls are expressed in dimensionless form by the Nusselt and Sherwood numbers:

$$Nu = \int_0^1 \left(\frac{\partial \theta}{\partial \xi}\right)_{\xi=0} d\eta \quad (7a)$$

$$Sh = \int_0^A \left(\frac{\partial \phi}{\partial \eta}\right)_{\eta=0} d\xi \quad (7b)$$

2.2. Method of solution

A control volume, finite-difference approach is used to solve the model equations with specified boundary conditions. SIMPLER algorithm is employed to solve the equations in primitive variables. Central difference is used to approximate advection-diffusion terms, i.e., the scheme is second order accurate in space. The governing

equations are converted into a system of algebraic equations through integration over each control volume. The algebraic equations are solved by a line-by-line iterative method. The method sweeps the domain of integration along the ξ and η-axis and uses tri-diagonal matrix inversion algorithm to solve the system of the algebraic equations. Fully implicit Euler method is used to update the solution in the time domain. The criteria of convergence are to conserve mass, momentum, energy and species globally and locally, and to insure convergence of preselected dependent variables to constant values within machine error at each time step.

In order to insure that the results are grid size independent, different meshes are tested namely 121×61, 161×81 and 201×101. The difference between predictions of using 121×61 and 161×81 grids was less than 1% in *Nu*, *Sh*, maximum U and V-velocity components at the mid plane of the enclosure. The difference between results obtained using 161×81 and 201×101 was less than 0.5%. Most calculations presented in this paper are performed using non-uniform 161×81 grids. Very fine grids are adopted near boundaries. These fine grids are necessary to resolve narrow channel flow, which is predicted for a range of controlling parameters. Also, influence of the time step effect is analyzed, the results are presented by using dimensionless time step of $\Delta\tau = 4 \times 10^{-4}$. Such a small time step is necessary to reduce aliasing effects (about 500 points for each frequency) and minimize numerical errors. Furthermore, the results in classical transient thermal natural convection are compared with Lauriat and Altimir [14] results and for thermosolutal convection the work of Tobbal and Bennacer [15] can be consulted.

3. NUMERICAL RESULTS AND DISCUSSION

The controlling parameters that define the fluid flow and heat and mass transfers for double diffusive natural convection in an enclosure are aspect ratio (A), Gr_T, Pr, N and Le. It needs quite extensive analysis to cover effects of each parameter. It is intended to limit the analysis for Prandtl number of 7.0 (water), $Le = 100$ as model of salt diffusion in water and for an aspect ratio of two as a horizontal enclosure which could be a practical size of pool energy storage.

Stable solutal stratified fluid resists flow evolution. On the other hand applying horizontal temperature gradient across the cavity initiates flow, even for a very small temperature gradient. Hence, there is a competition between thermal and solutal buoyancy forces. As N approaches zero, the thermal buoyancy drives the flow and formation a longitudinal recirculated flow is expected for moderately high *Ra* parameter. As N becomes much larger than the unity, the flow suppressed in the enclosure and diffusion dominates heat and mass transfer. Then *Nu* approaches 0.5 and *Sh* approaches 1.0 for aspect ratio of two, where the Nusselt and Sherwood parameters are based on the height of the enclosure. For N of order of unity, the competition between thermal and solutal buoyancy forces becomes same order of magnitude. Hence, the dynamic of the flow becomes more involved. Accordingly, the analysis is focused on this range of N parameter, i.e., N is of order of unity, specifically $0.5 \leqslant N \leqslant 10.0$.

The following sections discuss flow, thermal and species concentration structures, then bifurcation diagram and heat and mass transfer rates follow.

3.1. Flow, isotherms and isoconcentrations distributions

The results are generated for $Gr_T = 1 \times 10^3$, 1×10^4 and 1×10^5. The results are presented for $Gr_T = 1 \times 10^4$ and for different buoyancy parameters, and the discussion is qualitatively valid for $Gr_T = 1 \times 10^3$ and $Gr_T = 1 \times 10^5$.

The results for $Gr_T = 1 \times 10^4$ is shown in *figure 2(a)–(c)* for $N = 2.5$, 6 and 9, respectively. For $N = 2.5$, the flow is driven mainly by the thermal buoyancy force. The flow structure contains one main recirculation in the entire enclosure. Concentration gradient reversal is evidenced at the core of the cavity, due to strong flow circulation. Also, vertical thermal stratification is evidence at the core of the cavity. As the N value increases the strength of the flow circulation decreases and starts to bifurcate into smaller thermal central cell and upper and lower counter-wise rotating weak thermosolutal cells, *figure 2(b)*. The concentration reversal diminishes as N increases. For $N = 9$ (*figure 2(c)*) very weak flow is evidence near the horizontal boundaries and flow in the core becomes stagnant. The tilt of the isoconcentration induces solutal buoyancy forces that compensate the thermal forces. Due to the horizontal walls (confined domain) the tilt is difficult to sustain, hence weak horizontal cell forms. The flow channeling has an effect on the iso-concentration distributions at the left bottom corner and due to centro-symmetry at the upper right corner. The flow mechanism can be explained by the fact that,

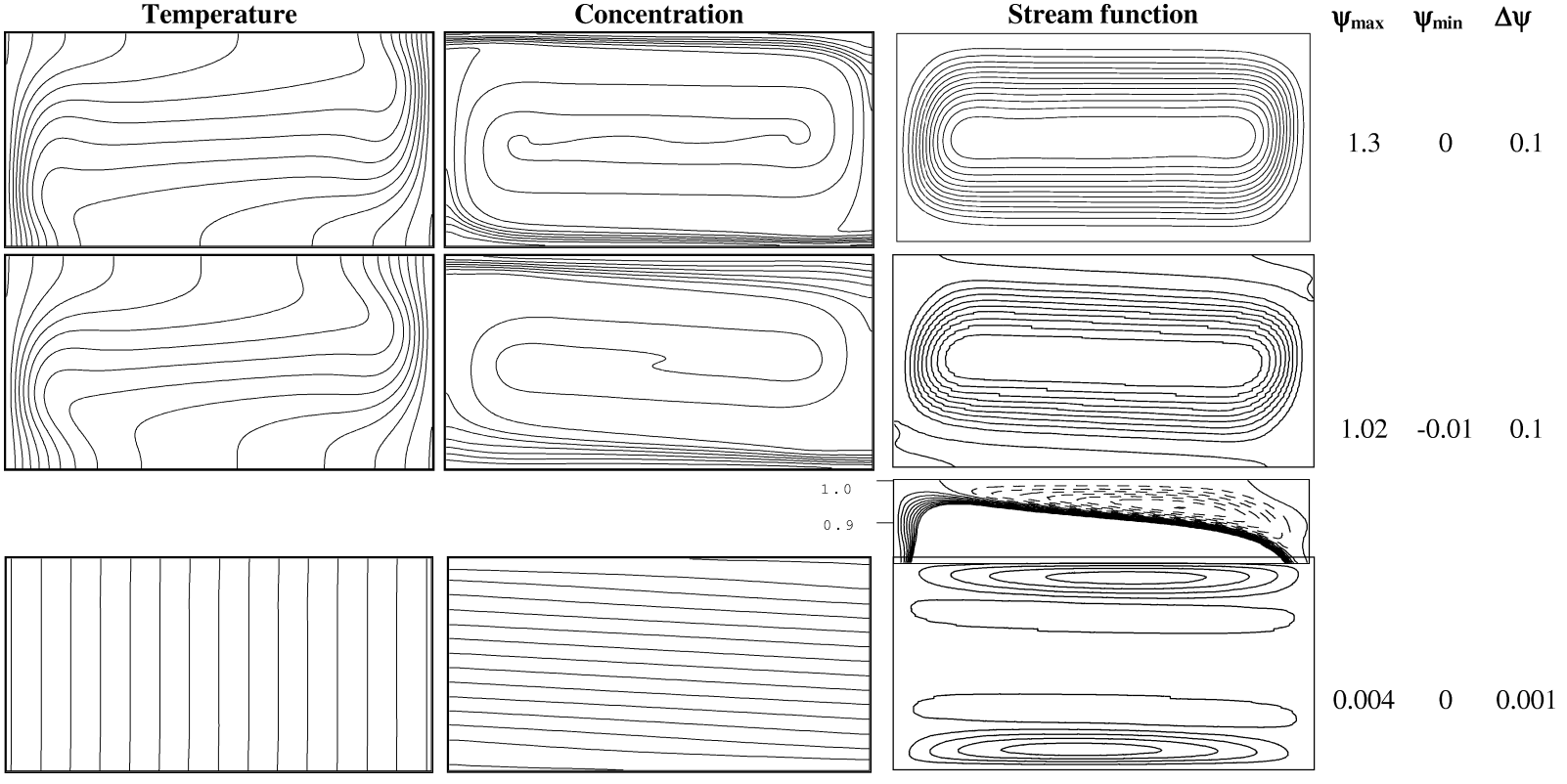

Figure 2. Streamlines, temperature and concentration contours for different buoyancy ratio: (a) $N = 2.5$; (b) $N = 6$; and (c) $N = 9$ $Gr_T = 10^4$, $Pr = 7$, $Le = 100$, $A = 2$.

the fluid in the left bottom corner becomes hot and rises, because of compensate concentration force, the flow suppressed away from the hot boundary and weak cell take place which permits parallel isoconcentration and inhabits the flow in the core. Similar discussion can be applied for the right top corner (cold boundary). As a conclusion three cases can be distinguished, a thermal convective regime for relatively small N ($N < 1$), a thermal and solutal diffusive regime with no significant flow for relatively high N value ($N > 8$) and a thermosolutal convective cell for moderated N value ($1 < N < 8$).

It is possible to obtain different solutions depending on the initial conditions. Also, flow instability can take place due to internal wave formation in a transitional domain and steady state solutions are not possible. These issues will be discussed in more details in the following paragraphs.

3.2. Heat and mass transfer hysterysis

A set of test is done in order to analyze the evolution of heat and mass transfer as a function of N. Two ways of exploration are adopted, the solution for a fixed N is obtained by initializing the calculation with a solution corresponding for higher N (diffusive solution) and for lower N (convective solution). *Figure 3* illustrates the heat and mass transfer evolution with N. As mentioned before for lower N, thermal convective cells take place and transfers are convective. The mass transfer is higher than the rate of heat transfer due to the higher value of the Lewis number (100); the species diffuse less than the heat. With increasing N the heat and mass transfers decrease because stable solutal stratification region take place without significant flow in the stratified domain. For N higher than 7.5 stable diffusive solution with relatively no flow in the entire cavity is obtained. Starting the solution from $N = 7.5$ (stabily stratified flow) and gradually decreasing N, the flow remains stable until N equal to about 3.5, where for N smaller than about 3.5, the convection regime take place. Similar hysterisys is obtained for higher N with increasing Gr_T. The existence of two possible solutions is also found in double diffusive problem with horizontal gradients (Nishimura et al. [16]). The ranges of N where two solutions are possible increase with increasing Gr.

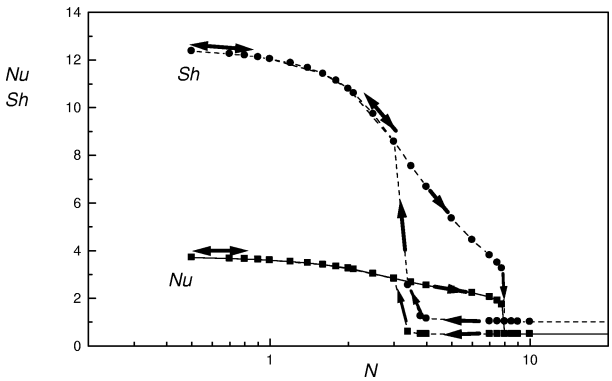

Figure 3. Effect of buoyancy ratio on Nusselt and Sherwood numbers $Gr_T = 10^4$, $A = 2$, $Pr = 7$, $Le = 100$.

In order to complete the numerical results and to be able to predict the heat and mass transfer an analytical approach is attempted as discussed in the following section.

4. ANALYTICAL SOLUTION

Let us consider the stratified zone in the upper part of the enclosure and let h^* be the height of this zone (*figure 4*). The velocity in the solutal stratification is very small and we may assume that the vertical variation of the concentration C is linear (*figure 5*). The concentration flux in the vertical direction is supposed to be extracted by the thermal flow in the central part (thermal cell) of the enclosure

$$\mathfrak{I} = D\frac{C_l - C_o}{h^*} \tag{8}$$

where C_l and C_o are, respectively, the concentration specified at the upper surface and the average value. Let ϑ_T to be the average horizontal velocity in the thermal loop, the order of magnitude of ϑ_T may be deduced from the thermal Rayleigh number based on the effective height of the thermal cell:

$$h_T = H - 2h^* = H(1-\varsigma) \quad \text{where } \varsigma = 2h^*/H$$
$$\vartheta_T \sim \frac{\alpha}{H} Ra_T^{1/2}(1-\varsigma)^{1/2} \tag{9}$$

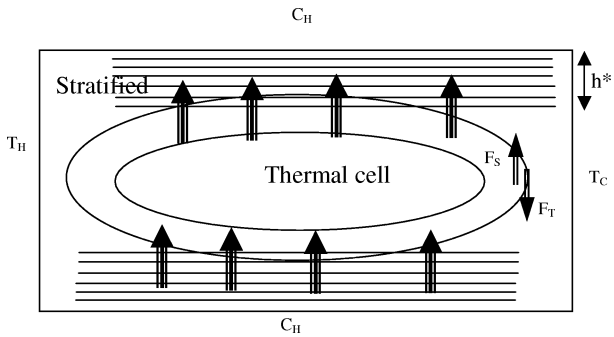

Figure 4. Schematic configuration.

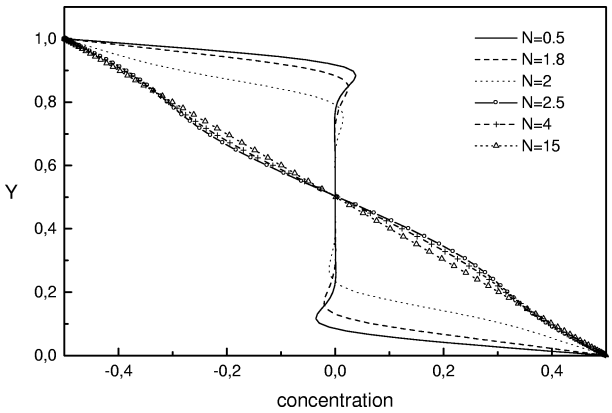

Figure 5. Concentration profile in the vertical mid plane.

and the dimensionless thermal boundary layer can be estimated as:

$$\delta_{\mathrm{T}} \sim Ra_{\mathrm{T}}^{-1/4}$$

During the average time for a fluid particle to cross the width of the enclosure, $\tau \approx L/\vartheta_{\mathrm{T}}$, the solute diffuses on a vertical length $Z \approx \sqrt{D\tau}$. The mass transfer rate between the stratified zone and the affected zone of thermal cell is: $\Im\tau\Delta x = \Delta C^* Z \Delta x$ where ΔC^* is the concentration increase, these lead to:

$$\Im = \Delta C^* Z/\tau = \Delta C^* \sqrt{D/\tau} \tag{10}$$

The system is in the steady state if the local thermal buoyancy term balances the local solutal force

$$\Delta\rho_{\mathrm{C}} \sim \Delta\rho_{\mathrm{T}} \tag{11}$$

with local solutal and thermal buoyancy forces are given by $\Delta\rho_{\mathrm{C}} \sim \beta_{\mathrm{S}}\Delta C^*$ and $\Delta\rho_{\mathrm{T}} \sim \beta_{\mathrm{T}}\Delta T H/\delta_{\mathrm{T}}$, respectively.

After manipulation equations (8)–(11), the following relationship is yield:

$$\varsigma(1-\varsigma)^{1/2} \sim N(Le/A)^{-1/2} Ra_{\mathrm{T}}^{-1/2} \tag{12}$$

where $A = L/H$.

Then, it is possible to estimate the minimum stratification height (ς) for any steady-state situation defined by the parameters N, Le, A and Ra_{T}. This analysis is not valid for oscillatory regime, or for very small stratification heights, where the hypothesis of linear vertical variation of the solute concentration is not adequate. So, in order to estimate the average heat and mass transfer as a function of the height of the compositional stratification, it can be consider that the rate of heat transfer is mainly due to the thermal cell in the centre of the cavity, which excludes the stratification regions. Then, the heat transfer may be estimated on the basis of a Rayleigh number based on the effective height of the thermal cell (with condition of distinct boundary layer), then

$$\overline{Nu} \sim Ra_{h_{\mathrm{T}}}^{1/4} \sim \overline{Nu}_{\mathrm{H}}(1-\varsigma)^{3/4} \tag{13}$$

where $\overline{Nu}_{\mathrm{H}}$, is the average heat transfer obtained when the thermal cell occupies the whole height of the enclosure (low values of N). The estimation of the Nusselt number is then possible due to the existence of heat transfer correlation in pure thermal convection case $\overline{Nu}_{\mathrm{H}} = 0.2Ra_{\mathrm{T}}^{11/40}$.

The Sherwood number is given by the dimensionless form of $\Im = (C_{\mathrm{l}} - C_{\mathrm{o}})/h^*$ which can be rewritten as

$$\overline{Sh} = \frac{1}{\varsigma} \tag{14}$$

Equations (12)–(14) may be used to estimate the decrease in heat and mass transfer. Besides, at a given Le and Gr_{T}, it is possible to determine the value of N corresponding to pure diffusive transfer.

The above analysis is useful in estimating the rate of heat and mass transfers as a function of buoyancy ratio. Also, the analysis illustrates the influence of the governing parameters on the rate of heat and mass transfers. The analysis is however restricted to the situation where a compositionally stratified zone is present in the top and bottom part of the enclosure and without oscillatory regime.

The comparison between numerical and theoretical results and the possible oscillating regime are presented in the next section.

5. HEAT AND MASS TRANSFER EVOLUTIONS

In order to compare the heat and mass transfer evolution versus N and for different Gr_{T} number, first the stratification height is estimated from equation (12). Then, the rate of mass transfer can be estimated from equations (13) and (14).

For thermal dominant flows (without stagnant stratified zone) $N \ll 1$ the mass transfer is not coupled with the momentum equation and mass transport equation can be solved for a given velocity field.

The numerical results can be used to evaluate the coefficient of equation (12), which can be rewritten as

$$49 \cdot \varsigma(1-\varsigma)^{1/2} \approx N(LeA)^{-1/2} Ra_{\mathrm{T}}^{-1/2} \tag{15}$$

The comparison between numerical and analytical results are given in *figure 6 (a)* and *(b)* for *Nu* and *Sh*, respectively.

The comparison between scale analysis and numerical results shows a good agreement for the three different *Gr* numbers and illustrates well the validity of the analytical estimation and the transition from thermal convective to fully diffusive regime. The value of N over which the diffusive transfer is obtained are also well estimated.

The difference is more profund on mass transfer, this is essentially due to the non linearity of the concentration at the horizontal inner cell interface and also due to sensitivity of species concentration to weak flow which occurs in the stratified domain.

As mentioned before, in the transitional regime the height of the stagnant stratified zone increases and some oscillating solution is obtained, this issue is the topic of the next section.

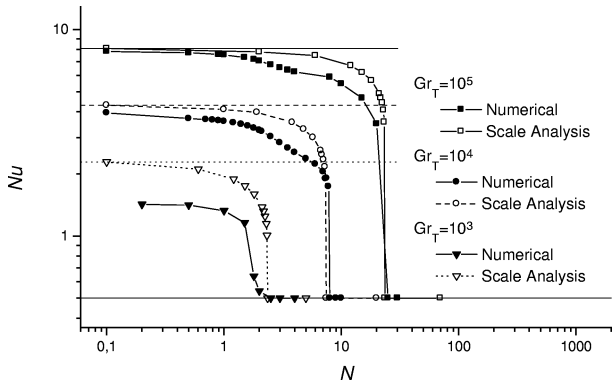

(a)

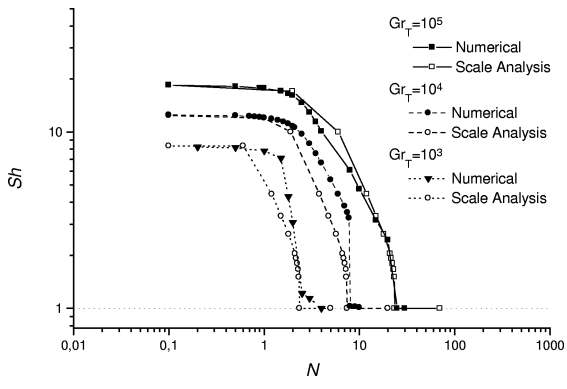

(b)

Figure 6. Comparison between Numerical and analytical results: (a) Average heat transfer on a vertical wall; (b) Average mass transfer on a horizontal mid plane.

6. OSCILLATORY REGIME

It is found that a periodic oscillatory flow appears for a certain range of buoyancy ratios. In order to illustrate the oscillations, results of oscillatory case is presented for $N = 10$ and $Gr_T = 10^5$, where steady state solution of $N = 8$ and $Gr_T = 10^5$ is used as initial value (at $\tau = 0$). *Figure 7* represents the average heat transfer on the mid-plane (a), which is given by $Nu = \int_0^1 (Pr\, u\theta - \partial\theta/\partial\zeta)\, d\eta$ and on the vertical wall (b). The amplitude of the oscillations is larger in the middle of the cavity than at the wall; this is essentially due to the importance of the advective term in the central oscillating cell.

Figure 8 (a) and *(b)* illustrate the oscillation of the average mass transfer on the horizontal mid-plane (a) and on the horizontal wall (b). The mass transfer shows weak oscillation on the wall (*figure 8(b)*) this is essentially due

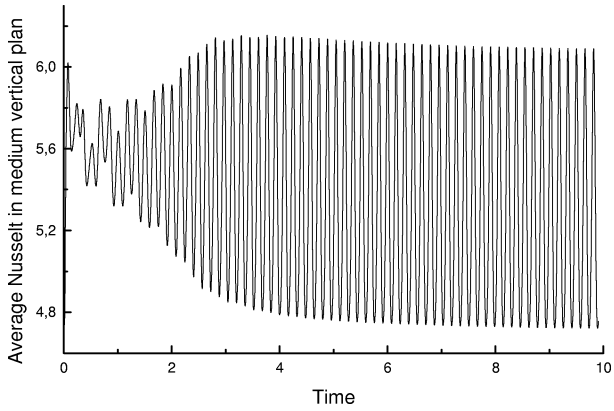

(a)

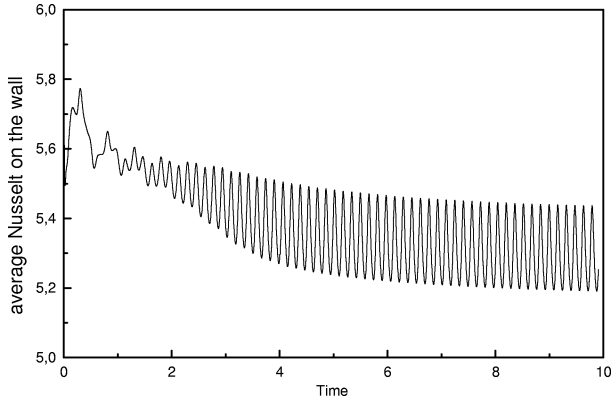

(b)

Figure 7. Temporal variation of the average heat transfer: (a) At the vertical mid plane; (b) On the wall $Gr_T = 10^5$, $N = 10$, $A = 2$, $Pr = 7$, $Le = 100$ (initializing by $N = 8$).

to the very thin solutal boundary layer ($Le = 100$) and the stabilizing effect of stratification, which is not strongly affected by the dynamic core oscillations. *Figure 8(a)* shows that the mass transfer amplitude oscillation is more than 50% of the average value, this tends to indicate that the oscillation is due to the adding solutal to the central thermal convective cell. It can be seen that the heat and mass transfer decrease with the increase of N (*figures 7* and *8*).

Fourier transform of the time evolution of the average Sherwood number (*figure 8*) is represented on *figure 9*. This figure illustrates that the dominant dimensionless frequency is 8.6, which is physically due to thermal and solutal competition. Moreover, the flow patterns are plotted during one period of the oscillation. Five instants over one period and the corresponding streamlines, temperature and concentration fields are shown in *figure 10*.

Figure 10(a) illustrates the phase difference between the stream function, heat and mass transfer. The phase difference between heat and mass transfer is due in part to difference in localization boundary conditions between temperature (vertical walls) and concentration (horizontal wall); they sense the excitation after different time interval.

The streamlines (*figure 10(b)*) shows a strong inner cell which is essentially due to thermal forces and very weak counter-clock cell in the upper and lower domain of the cavity. This cell is stabilized by the solutal

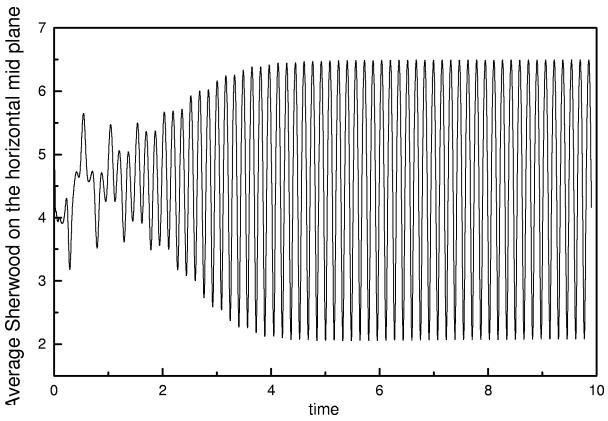

(a)

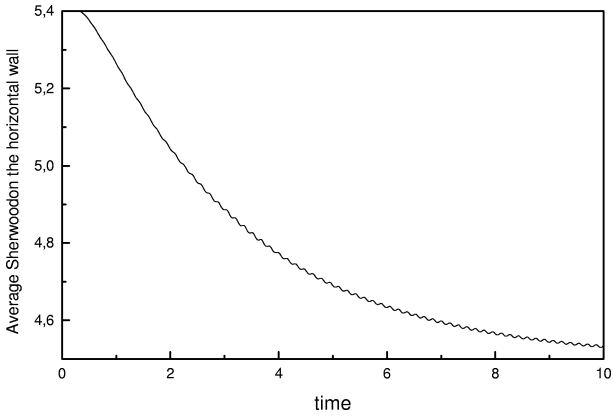

(b)

Figure 8. Temporal variation of the average mass transfer: (a) At the horizontal mid plane; (b) On the horizontal surface $Gr_{\mathrm{T}} = 10^5$, $N = 10$, $A = 2$, $Pr = 7$, $Le = 100$ (increasing case from $N = 8$).

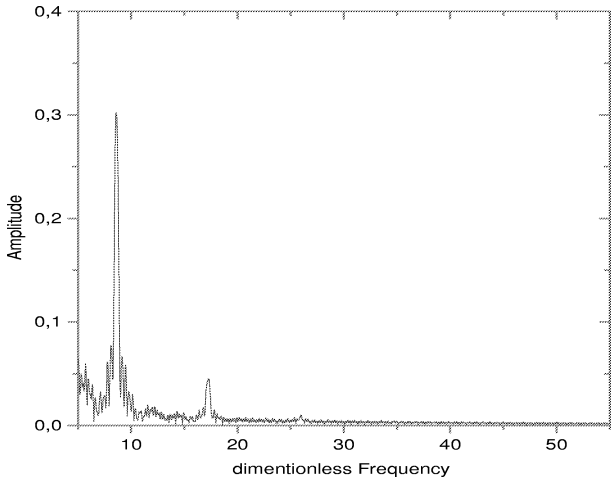

Figure 9. Power spectrum of Sherwood oscillation $Gr_{\mathrm{T}} = 10^5$, $N = 10$, $A = 2$, $Pr = 7$, $Le = 100$ (increasing case from $N = 8$).

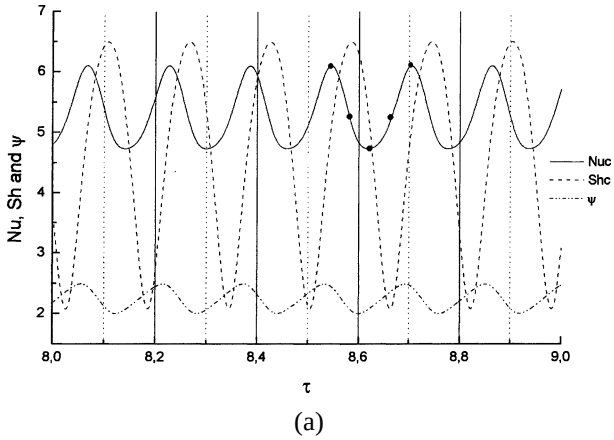

(a)

Figure 10. Temporal variation of flow: (a) The positions of five instants in one period; (b) Flow, temperature and concentration field for $Gr_{\mathrm{T}} = 10^5$, $N = 10$, $A = 2$, $Pr = 7$, $Le = 100$ (increasing case from $N = 8$).

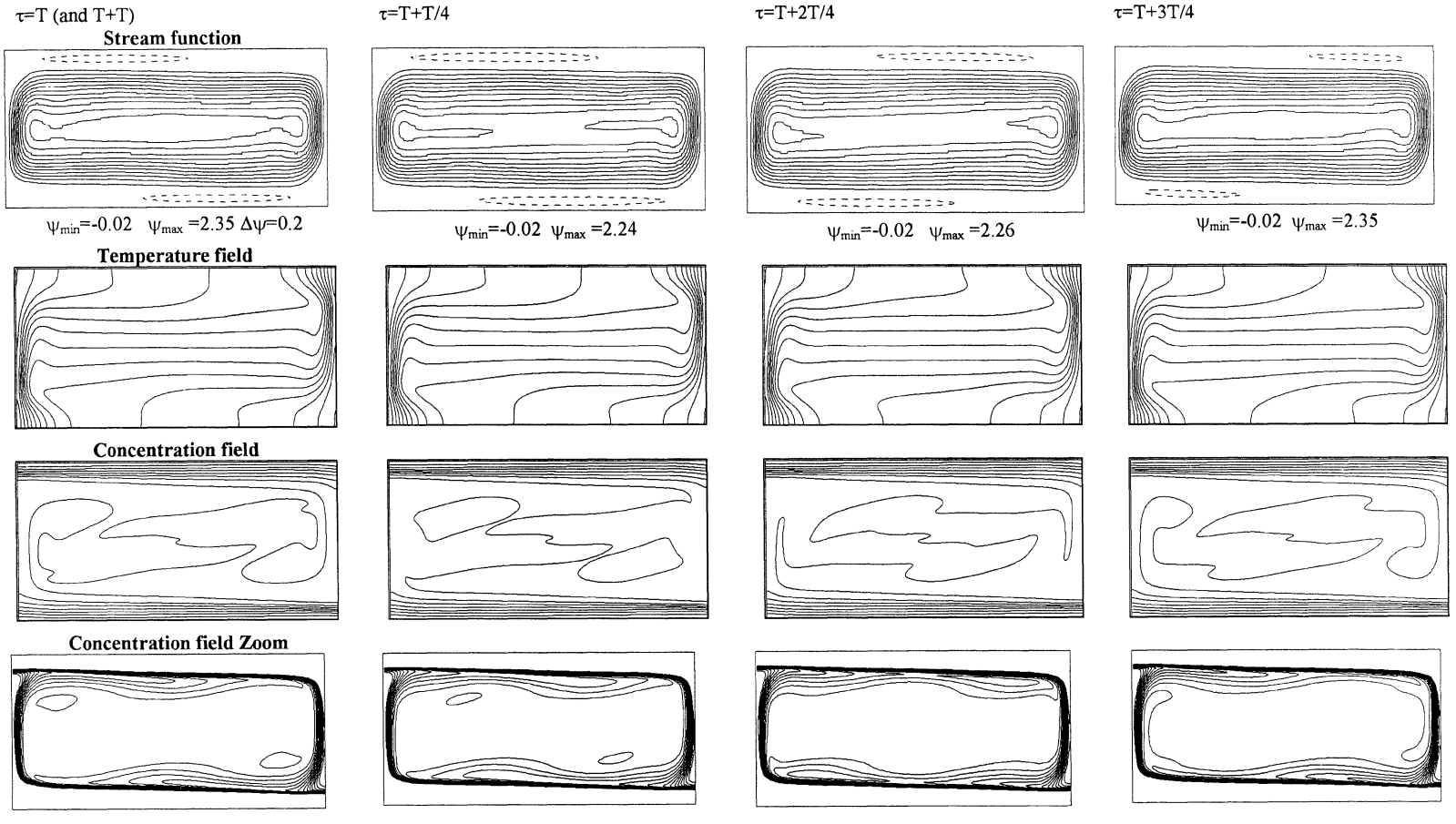

(b)

Figure 10. (continued).

stratification. The rotation is due in part to the inner cell viscous effect and to solutal forces. It can easily be seen that the oscillation is essentially due to unstable center of the inner cell where solutal plums take place and perturb the inner cell. This plum is as a result of inversion in the concentration field. A zoom in concentration field illustrates well the surface thermal-solutal interface wave and the lower (higher) density fluid, which is ejected near the cold (hot) wall.

The mechanism of plume existence can be summarized as:

(1) solute diffuse from top (bottom) to the inner cell during the average time for a fluid to cross the width of the enclosure,

(2) the affected region is dragged by viscous effect to the bottom (top) of the cavity,

(3) the species affect by diffusion a large domain and when the viscous forces decreases (in the bottom right corner) the solutal dragged region becomes unstable,

(4) the solutal force pulls up plums and passes through the inner cell and perturbs the general flow.

There is a strong interaction between the lower and the upper part of the oscillating inner cell where it can be evidenced from an ascending plum contribute in the creation of the descendant one.

The phase difference between heat transfer and inner cell intensity is relatively small because the inner cell is due to thermal field.

7. CONCLUSION

The natural convection in an enclosure with horizontal temperature gradient and vertical concentration gradient was examined numerically and analytically. The effect of buoyancy ratio was considered under the condition $Pr = 7.0$, $Le = 100$ and $A = 2.0$. The following conclusive remarks have been drawn.

(1) It is found that there are three distinct regimes, for lower N value the convective cell is essentially due to thermal forces, for high N value the transfer is diffusive and the stabilizing solutal stratification suppresses the flow and intermediate domain (moderate N value) the transfer decreases with N.

(2) The scale analysis permits to evaluate the mass and heat transfer and the critical N above which connective solution is possible. However, the scale analysis fails to predict the hysterysis.

(3) The comparison between scale analysis and numerical results evidences a good agreement. Difference is more important on mass transfer, this is essentially due to the non-linearity of the concentration at the horizontal inner cell interface and sensitivity species concentration to weak flow, which occurs in the stratification.

(4) In the transitional flow regime, the numerical solution is found to depend on the initial condition. Flow hystresis effects are observed and two distinct solutions are present for a given buoyancy ratio.

(5) Oscillatory flow takes place in a limited range of buoyancy ratios and is due to solutal plume and alternative exchange between the inner thermal cell and the stable concentration stratification.

REFERENCES

[1] Bejan A., Convection Heat Transfer, Wiley, New York, 1984.

[2] Krishnan, A numerical study of the instability of double-diffusive convection in a square enclosure with horizontal temperature and concentration gradients, in: National Heat Transfer Conference: Heat Transfer in Convective Flows, Vol. 107, 1989, pp. 357–368.

[3] Zhou, Zebib A., Oscillatory double diffusive convection in crystal growth, J. Crystal Growth 135 (1994) 587–593.

[4] Gobin, Bennacer, Double diffusion in a vertical fluid layer: Onset of the convective regime, Phys. Fluid 6 (1994) 59–67.

[5] Kamakura, Ozoe H., Double diffusive natural convection in a rectangle with horizontal temperature and concentration gradients, in: Thermal Engineering Conference, Vol. 1, 1995, pp. 171–178.

[6] Nishimura, Imoto T., Wakamatsu M., A numerical study of the structure of double diffusive natural convection in square cavity, in: Thermal Engineering Conference, Vol.1 ASME, 1995, pp. 193–200.

[7] Mohamad A.A., Bennacer R., Natural convection in a confined saturated porous medium with horizontal temperature and vertical solutal gradients, Internat. J. Thermal Sci. 40 (1) (2001) 82–93.

[8] Thorpe S.A., Hutt P.K., Soulsby R., The effect of horizontal gradients on thermohaline convection, J. Fluid Mech. 38 (1969) 375–400.

[9] Wirtz, Reddy C.S., Experiments on convective layer formation and merging in a differentially heated slot, J. Fluid Mech. 91 (1979) 451–464.

[10] Bénard R.B., Bennacer R., Gobin D., Melting driven thermohaline convection, Phys. Fluids 8 (1996) 112–130.

[11] Chen, Liou J.K., Time-dependent double diffusive convection due to salt-stratified fluid layer with differential heating in an inclined cavity, Internat. J. Heat Mass Transfer 40 (1997) 711–725.

[12] Dijksta A., Kranenborg E.J., On the evolution of double diffusive intrusions into stabily stratified liquid: the physics of self-propagation, Internat. J. Heat Mass Transfer 14 (1998) 2113–2124.

[13] Hollinger St., Lücke M., Influence of the Soret effect on convection of binary fluids, Phys. Rev. E 57 (1998) 4238–4249.

[14] Lauriat G., Altimir I., A new formulation of SADI method for the prediction of natural convection flows in cavities, Comput. Fluids 13 (1985) 141–155.

[15] Tobbal A., Bennacer R., Heat and mass transfer in anisotropic porous layer, Res. Trend Heat Mass and Momentum Transfer 3 (1998) 129–137.

[16] Nishimura, Wakamatsu M., Morega A., Oscillatory double-diffusive convection in a rectangular enclosure with combined horizontal temperature and concentration gradients 41 (1998) 1601–1611.